arXiv:astro-ph/0112500v1 20 Dec 2001

Interstellar Hα Line Profiles toward HD 93521 and the Lockman Window

N. R. Hausen, R. J. Reynolds, L. M. Haffner

Department of Astronomy, University of Wisconsin–Madison

475 North Charter Street, Madison, WI 53706

hausen@astro.wisc.edu, reynolds@astro.wisc.edu, haffner@astro.wisc.edu

and

S. L. Tufte

Department of Physics, Lewis & Clark College

0615 SW Palatine Hill Road, Portland, OR 97219

tufte@lclark.edu

ABSTRACT

We have used the Wisconsin Hα Mapper (WHAM) facility to measure the interstellar Hα emission toward the high Galactic latitude O star HD 93521 ($\ell = 183\overset{\circ}{.}1$, $b = +62\overset{\circ}{.}2$). Three emission components were detected along this line of sight. These components have radial velocities of –10 km s^{-1}, –51 km s^{-1}, and –90 km s^{-1} with respect to the local standard of rest (LSR) and have Hα intensities of 0.20 R, 0.15 R, and 0.023 R, respectively, corresponding to emission measures of 0.55 cm^{-6} pc, 0.42 cm^{-6} pc, and 0.06 cm^{-6} pc. We have also measured the Hα emission toward the direction $\ell = 148\overset{\circ}{.}5$, $b = +53\overset{\circ}{.}0$, which lies in the region of exceptionally low H I column density known as the Lockman Window. An emission component is detected in this direction at –1 km s^{-1} (LSR) with an intensity of 0.20 R (0.55 cm^{-6} pc). In addition, we studied the direction $\ell = 163\overset{\circ}{.}5$, $b = +53\overset{\circ}{.}5$. No Galactic emission was detected along this line of sight, and upper limits on the possible intensity of Galactic emission toward this direction are 0.11 R at the LSR and 0.06 R at –50 km s^{-1}. As part of the process of separating the interstellar from the terrestrial emission, we also detected and characterized twelve faint ($\sim$0.03-0.15 R), unidentified atmospheric lines present in WHAM Hα spectra. Lastly, we have used WHAM to obtain [O I] λ6300 spectra along the line of sight toward HD 93521. We do not conclusively detect

interstellar [O I] emission toward the star, but place an upper limit of 0.060 R on the [O I] intensity of the intermediate velocity (–51 km s^{-1}) component. If the temperature of the gas is 10,000 K, this limit implies that within the Hα emitting region, the hydrogen ionization fraction $n(H^+)/n(H_{total}) > 0.6$.

Subject headings: ISM: atoms — ISM: clouds — ISM: general — stars: individual (HD 93521)

1. INTRODUCTION

The Wisconsin Hα Mapper (WHAM) is a dual-etalon, Fabry-Perot spectrometer designed to measure optical emission from diffuse interstellar sources. WHAM is approximately 100 times more sensitive than the previous instrument of its kind, making it possible to study very low levels of emission not accessible in the past. The WHAM Hα studies presented in this paper were made along three lines of sight in which the interstellar Hα emission is extremely faint. In particular, we have measured the Hα emission line profile toward HD 93521 ($\ell = 183\overset{\circ}{.}1$, $b = +62\overset{\circ}{.}2$), supplementing the work of Spitzer & Fitzpatrick (1993), who obtained ultraviolet *HST* absorption line measurements for numerous species toward this star. Secondly, we have measured the Hα emission toward $\ell = 148\overset{\circ}{.}5$, $b = +53\overset{\circ}{.}0$, which lies in the region of sky known as the Lockman Window. This region has the lowest H I column density of any section of the northern sky, and thorough 21 cm studies of the area have been made by Jahoda, Lockman, & McCammon (1990) and Lockman, Jahoda, & McCammon (1986). The Hα observations provide information about the amount of H II in this unusual direction. Lastly, we have observed the line of sight toward $\ell = 163\overset{\circ}{.}5$, $b = +53\overset{\circ}{.}5$ (referred to below as "Off A"). This direction was selected for investigation based on WHAM Northern Sky Survey data, which indicated that only minimal levels of Hα emission could be present. Results for these three directions are discussed in §3.4, §3.3, and §3.2, respectively.

Accompanying WHAM's ability to detect faint *Galactic* emission is its ability to detect faint *terrestrial* emission lines as well. In fact, WHAM Hα spectra centered near the local standard of rest (LSR) show a total of twelve weak ($\sim$0.03 – 0.15 R, 1 R = $10^6/4\pi$ photons cm^{-2} s^{-1} sr^{-1}) sky lines of unknown origin in addition to the well known and much brighter geocoronal Hα line. These weak lines are present at fixed positions with respect to the geocoronal line, and their intensities vary slightly during the night. Of these twelve lines, four on the blue side of the geocoronal line were first noticed in WHAM spectra used to study high-velocity clouds and are discussed by Tufte et al. (1998) and by Tufte (1997). One of the lines to the red of the geocoronal line is discussed by Haffner, Reynolds, & Tufte

(1998). Since the atmospheric lines can significantly affect measurements of faint Galactic Hα emission, it is important to understand and remove their contributions to the data. In §3.1, we give a characterization of the twelve faint atmospheric lines based on a study of a large sample of WHAM Hα spectra.

In addition to Hα other, fainter emission lines can provide information about the physical state of the emitting gas. For example, measurements of Galactic [O I] λ6300 emission along a given line of sight, when combined with the Hα intensity for that direction, yield information regarding the ionization state of the emitting gas, a subject of interest and some controversy for the HD 93521 sightline (e.g., Spitzer & Fitzpatrick 1993; Slavin, McKee, & Hollenbach 2000). In particular, the hydrogen ionization ratio $n(\mathrm{H}^+)/n(\mathrm{H}^\circ)$ in the gas can be obtained via the observed [O I]/Hα line intensity ratio. The precise relation, as given by Reynolds et al. (1998) and references therein, is

$$\frac{I_{[\mathrm{O\ I}]}}{I_{\mathrm{H}\alpha}} = 2.74 \times 10^4 \left(\frac{T_4^{1.854}}{1 + 0.605 T_4^{1.105}} \right) \exp\left(-\frac{2.284}{T_4} \right) \frac{n(\mathrm{O})}{n(\mathrm{H})} \left[\frac{1 + n(\mathrm{H}^\circ)/n(\mathrm{H}^+)}{1 + (8/9) n(\mathrm{H}^+)/n(\mathrm{H}^\circ)} \right], \quad (1)$$

where $I_{[\mathrm{O\ I}]}/I_{\mathrm{H}\alpha}$ is the intensity ratio measured in energy units and T_4 is the electron temperature in units of 10^4 K. The term $n(\mathrm{O})/n(\mathrm{H})$ is the gas-phase abundance of oxygen, which we take to be 3.2×10^{-4} (Meyer, Jura, & Cardelli 1998). The [O I] observations are discussed in §3.5 and §4.

2. OBSERVATIONS

The Wisconsin Hα Mapper facility consists of a 15 cm aperture, dual-etalon, multichannel Fabry-Perot spectrometer attached to a 0.6 m siderostat. WHAM has a 1° beam on the sky and 12 km s^{-1} radial velocity resolution over a 200 km s^{-1} spectral range. This 200 km s^{-1} interval can be centered on any wavelength between 4800 and 7300 Å. A more detailed description of this instrument and its operation is provided by Tufte (1997) and Haffner (1999). WHAM is a remotely-operable facility located at Kitt Peak National Observatory, and all observations for this paper were obtained remotely from Madison, WI.

2.1. Hα

An "on-off" technique similar to that described by Tufte et al. (1998) was used to determine the interstellar Hα emission line profiles toward HD 93521 and the Lockman Window. With this method, exposures toward the direction of interest (the "on") are alternated with exposures toward an "off" direction in which the Galactic emission is significantly weaker.

The "off" spectra are then subtracted from the "on" spectra, thereby removing, or at least significantly reducing, all features common to the two directions, including the geocoronal Hα line, other much fainter terrestrial emission lines, and the weak Hα Fraunhofer absorption line in the zodiacal light.

A summary of Hα observations is given in Table 1. Each "on" spectrum and each "off" spectrum had an exposure time of 600 s, except the Lockman Window spectra noted in Table 1. HD 93521 is the "on" direction in Data Sets 1a,b,c, 3, and 7. The Lockman Window is the "on" direction in Data Sets 5 and 6. For the HD 93521 observations that used the Lockman Window as the "off," the "on-off" technique was complicated by the presence of a significant amount of Galactic emission toward the Lockman direction. Our correction for this is discussed in §3.4. When "Off A" was used (Data Sets 5, 6, and 7), no correction for Galactic emission was made, because the Galactic emission in this direction is below the detection limit of these observations (see §3.2). In addition, observations were repeated at different times of the year in order to utilize the shifting positions of the Galactic emission relative to the fixed positions of the atmospheric lines present in the spectra. Consistency between results was used as a check that the detected emission was Galactic in origin and not the result of contamination from the atmospheric lines.

2.2. Faint Atmospheric Lines near Hα

Our characterization of the faint atmospheric lines is based primarily on a study of more than eighty 60 s spectra toward the Lockman Window, taken on roughly 20 nights spanning a 14-month period in 1997 and 1998. Of these spectra, approximately half had the geocoronal line positioned on the red side of WHAM's 200 km s^{-1} spectral range, while the other half had the geocoronal line on the blue side of the spectrum. These data were gathered routinely during observing sessions for the WHAM Northern Sky Survey. In addition, we made use of many of the Lockman Window spectra listed in Table 1, including the spectra (each 600 s exposures) in Data Sets 2a,b and 4a,b.

Obtaining Lockman Window spectra over many months was important to our being able to separate the Galactic from the terrestrial emission, since at any one time, the Galactic emission near the LSR blends with one or more of the atmospheric lines, which have intensities comparable to that of the interstellar Hα. Over the course of the year, the position of the Galactic emission moves relative to the positions of the terrestrial lines, making the detection of the Galactic emission possible. In the process we were also able to characterize the atmospheric lines in the spectrum.

We also studied numerous high-latitude "blocks" taken from the WHAM Survey data (Haffner et al. 2002; also see `http://www.astro.wisc.edu/wham/`). Each block was the average of about forty nine 1° pointings (each with 30 s of exposure time) covering a roughly $6° \times 7°$ region of sky. These blocks contained only low levels of Galactic emission, making it possible to independently test the results from the Lockman Window studies. This assured us that the atmospheric line parameters that we had determined were not influenced by the Galactic emission toward a particular direction.

2.3. [O I] λ6300

Two bright atmospheric lines, the [O I] airglow line and an OH line at 6297.9 Å, are present in the [O I] λ6300 spectra, making the detection of faint Galactic [O I] emission quite difficult. The [O I] λ6300 studies for HD 93521 were therefore also based on the "on-off" method. Furthermore, for comparison purposes, observations were repeated at different times of year as the position of the Galactic emission shifted with respect to the terrestrial lines. Table 2 lists the observations. The Lockman Window is the "off" direction for Data Sets 8a,b, 9a,b, and 10a,b, whereas Data Set 11 uses Off A as the "off." With the exception of the Lockman Window spectra noted in Table 2, all individual spectra were 600 s exposures. Spectra in Data Set 11 were taken in an "on"/"off" sequence like that described for the Hα Data Sets (see §2.1). Data in the remaining [O I] Data Sets were gathered in the repeated sequence "on," "off," "on," yielding twice as much integration time for the "on" direction as for the "off."

3. RESULTS

3.1. Faint Atmospheric Lines near Hα

We detected twelve weak atmospheric lines in the WHAM Hα spectra centered near the local standard of rest. Figure 1, plotted with respect to the earth's velocity frame, shows the atmospheric lines that are visible when the geocoronal line is on the red side of the spectrum. The spectrum in Figure 1 is the sum of all Lockman Window spectra in Data Sets 1a,b,c, 3, 4a,b, and 5, normalized to 600 s. In each of the Data Sets 1, 3, 4, and 5, the Lockman Window Galactic emission near the LSR (discussed in §3.3 below) appears at a different geocentric velocity. Hence, this Galactic emission was removed from each of the constituent spectra before summing. Figure 2, also plotted with respect to the earth's velocity frame, shows a different wavelength region, with the geocoronal line located on the blue side of the

spectrum. This spectrum is the sum of all Lockman Window spectra in Data Sets 2a,b and 6, normalized to 600 s. Again, the Galactic emission has been removed from this spectrum.

Parameters for the faint atmospheric lines are given in Table 3. The low intensity and close spectral proximity of the lines made it difficult to fit them using free position, width, and intensity parameters. A fixed width of 10 km s^{-1} was therefore adopted for all lines except those numbered 4 and 10. The width was fixed at 15 km s^{-1} for Lines 4 and 10, which appear broader than the other lines. Line 10 may in fact be a blend of two components, as some spectra show a narrower-than-usual line with the position shifted by approximately 0.05 Å from the typical position of Line 10. It is possible that the remaining lines are also blends that WHAM does not resolve. Since the feature labeled in Figure 2 as Line 7a appeared to be present in only a very limited number of spectra, we did not characterize it in the same manner as the other atmospheric lines (see Table 3). We have not identified the atomic or molecular source of any of the weak atmospheric lines.

Table 3 gives the intensity of the lines as shown in Figures 1 and 2. The lines that are common to both Figure 1 and Figure 2 illustrate the degree to which the relative intensities of the lines can vary. For example, Line 6 is not detected in Figure 2, and Line 7a is not detected in Figure 1. We have found that, in general, absolute intensities are quite stable (< 0.05 R) over periods of a half hour or more. Furthermore, the relative intensities between lines are consistent enough for us to use a set of "adopted relative intensities", and these are given in Table 3. In a given spectrum, the adopted intensity for each line is a percentage of the intensity of Line 5 in that spectrum. The intensity of Line 5 itself is obtained from a Gaussian fit to the spectrum.

3.2. The "Off A" Direction

During reduction of the WHAM Northern Sky Survey, the Off A direction ($\ell = 163\overset{\circ}{.}5$, $b = +53\overset{\circ}{.}5$) was identified as having an exceptionally low level of Hα emission. Subsequent long exposures toward this direction have confirmed this (Data Set 5, in which the LSR is maximally to the blue of the geocoronal line for this direction). Although we detected no Galactic Hα emission toward this direction, we are ultimately limited by the presence of the geocoronal line and by uncertainties in the intensities of the faint atmospheric lines. Table 4 lists the resulting upper limits placed on possible Galactic emission toward the Off A direction from 0 to –50 km s^{-1}. We derived these limits using Data Set 5 spectra and assuming that three sources of uncertainty in our knowledge of the weak atmospheric lines (the absolute intensity of Line 5, the exact intensity ratios in a given spectrum between Line 5 and the other lines, and the uncertainty as to the presence of Line 6) all add positively in

the same direction.

3.3. Interstellar Hα Toward the Lockman Window

The spectra in Data Set 5 were used to determine the interstellar Hα emission line profile for the Lockman Window direction. Specifically, the six 600 s Off A spectra in Data Set 5 were averaged and then subtracted from the average of the six 600 s Lockman Window spectra in the same Data Set. The resulting spectrum is shown in Figure 3. In this figure, the subtraction residual of the geocoronal line (at +21 km s^{-1}) has been removed. Results from fits of the LSR component in this spectrum are listed in Table 4. The error bars in the table result from baseline uncertainties and the blend of the Galactic emission with the geocoronal line residual. For the intensity of the –1 km s^{-1} component, there is an additional systematic uncertainty (not included in Table 4) of +0.11 R, resulting from the upper limit on Galactic emission toward the Off A direction. We also derived the Galactic Hα spectrum toward the Lockman Window by subtracting Lockman Window spectra obtained in November (when the LSR is at –26 km s^{-1} wrt the earth) from Lockman Window spectra obtained in April (when the LSR is at +15 km s^{-1} wrt the earth). This difference spectrum greatly reduced the atmospheric features and revealed the Galactic emission as negative and positive spectral features near –26 km s^{-1} and +15 km s^{-1} respectively, with respect to the earth. The parameters for the Galactic emission derived from this technique were consistent with those derived using the Off A direction, indicating that the interstellar emission toward Off A is indeed less than 0.1 R.

For comparison, Figure 3 also shows the H I profile toward the Lockman Window. This spectrum is from the Leiden/Dwingeloo survey (Hartmann & Burton 1997), and is the average of their 0.°5 pointings whose centers fall within WHAM's 1° beam directed at $\ell = 148.°5$, $b = +53.°0$. Since the H I spectrum has an obvious component at –54 km s^{-1}, an upper limit in the Hα at this velocity was determined. The limit, given in Table 4, is based on fits to Lockman Window spectra at various times of the year. For these fits, a component was fixed in the spectra at –54 km s^{-1} with a width of 25 km s^{-1}. Different possible values of atmospheric line intensities were then considered in order to establish the Galactic emission upper limit listed in Table 4.

Lastly, two noticeable features in the Lockman Window Hα spectrum should be mentioned: the elevated data points near +60 km s^{-1} and the rise in the data at the negative edge of the spectrum. These features are within the baseline uncertainty of the spectrum and have no apparent correspondence in H I. It is nevertheless possible that one or both represent very low-intensity Galactic Hα emission. If the true baseline is near zero in the Figure 3 spec-

trum, then the positive-velocity feature is centered at about +56 km s^{-1} with an intensity of 0.04 R. The spectra in Data Set 6 were obtained in an attempt to verify whether this is a real Galactic emission component. Unfortunately, because the atmospheric lines near the region of interest showed marked intensity fluctuations between temporally-adjacent 600 s spectra in Data Set 6, we were unable to verify the reality of this weak feature.

No additional data were obtained to test whether the feature at the negative edge of the spectrum is indeed a high-velocity Galactic emission component. However, while using the Lockman Window as an "off" direction during a study of emission from high-velocity clouds, Tufte (1997) found evidence for the presence of a very weak emission component toward the Lockman Window near –130 km s^{-1}. This lends support to the idea that the feature in Figure 3 is Galactic in origin, but clearly further "on" minus "off" observations centered at a high, negative velocity would be needed to provide a definitive result.

3.4. Interstellar Hα Toward HD 93521

"On-off" studies of the spectra in Data Sets 1a,b,c and 3 reveal three interstellar Hα emission components toward HD 93521. There is a "slow" component at –10 km s^{-1}, an "intermediate velocity" component at –51 km s^{-1}, and a fainter, "high velocity" component at –90 km s^{-1}. Full results are given in Table 4. The error bars given in Table 4 for HD 93521 incorporate uncertainties associated with the baseline level and the blend of the slow component with the residual of the incompletely-subtracted geocoronal line. They also include the uncertainty generated by the error bars of the –1 km s^{-1} Lockman emission. The results in Table 4 do not include a systematic uncertainty of +0.11 R at the LSR, due to the upper limit on the Galactic emission toward Off A, or a systematic uncertainty of +0.06 R at –50 km s^{-1}, due to the upper limit on the Galactic emission at –50 km s^{-1} toward the Lockman Window.

The analysis conducted to obtain the results presented in Table 4 proceeded as follows: The five 600 s Lockman Window spectra in Data Sets 1a,b,c were averaged together, and the Galactic emission at –1 km s^{-1} (parameters given in Table 4) was removed from the average spectrum. It was assumed that there was no other Galactic emission in the Lockman Window spectra. The corrected average "off" spectrum was then subtracted from the average of the five 600 s HD 93521 spectra in Data Sets 1a,b,c. A similar procedure was followed for the data in Data Set 3, with the additional step of normalizing the average Lockman Window spectrum to 600 s of exposure time. Both "on-off" spectra were then studied, although parameters for the slow emission component were determined from the data in Data Sets 1a,b,c only, as the slow component was farthest from the incompletely-subtracted geocoronal

line in this case. During the Data Set 3 analysis, the parameters of the slow component were fixed at the best-fit values derived from Data Sets 1a,b,c.

As a check on these results, the spectra in Data Set 7 (for which Off A is the "off" direction) were also analyzed using the "on-off" method. This work was carried out under the assumption that there was no Galactic emission present in the Off A spectra. Also, because the Galactic emission near the LSR was blended with the incompletely-subtracted geocoronal line, parameters for the slow emission component were fixed during the analysis at the best-fit values given for this component in Table 4. The intermediate velocity emission component was then detected at –53 km s^{-1}, with a width of 31 km s^{-1} and an intensity of 0.13 R. The high velocity emission component was detected at –86 km s^{-1}, with a width of 20 km s^{-1} and an intensity of 0.022 R. These results are generally consistent with the uncertainties listed in Table 4, except for the best-fit width of the intermediate velocity component, which is slightly outside the error bars of the value derived from the study that used the Lockman Window as the "off." It is possible that this discrepancy is due to very low levels of undetected Galactic emission in the Lockman Window and/or Off A directions. Such emission may produce effects of this magnitude in the "on-off" line profile of an "on" direction in which the Galactic emission is faint.

Figure 3 shows the Hα profile toward HD 93521. This profile was obtained from the spectra in Data Sets 1a,b,c and 3. Specifically, the residuals from the incompletely-subtracted geocoronal line were removed from the two "on-off" spectra generated from these Data Sets. (These residuals were located at +26 km s^{-1} in the spectrum from Data Sets 1a,b,c and at +14 km s^{-1} in the Data Set 3 spectrum.) Then the two resulting spectra were averaged, yielding the spectrum given in Figure 3. Due to the LSR velocity off-set between 1997 November (Data Sets 1a,b,c) and 1999 January (Data Set 3), several data points at the positive velocity extreme in the November data and at the negative velocity extreme in the January data were unmatched with points in the other spectrum. These points were excluded from the average spectrum, and hence the velocity scale of the HD 93521 Hα spectrum in Figure 3 covers only a 188 km s^{-1} (rather than 200 km s^{-1}) interval.

Figure 3 shows the H I spectrum toward HD 93521 as well. The H I spectrum is the average of the Leiden/Dwingeloo pointings whose centers fall within WHAM's 1° beam directed at $\ell = 183\overset{\circ}{.}1$, $b = +62\overset{\circ}{.}2$. The H I spectrum has the same 188 km s^{-1} velocity scale as the HD 93521 Hα spectrum.

3.5. A Search for Interstellar [O I] λ6300 Emission Toward HD 93521

The strength of the [O I] emission relative to Hα is a measure of the hydrogen ionization fraction in the emitting gas and thus has the potential to test the conclusion of Spitzer & Fitzpatrick (1993) that the warm ionized gas toward HD 93521 is mixed with the H I, forming partially ionized (30%) clouds. Unfortunately, because it is so much weaker than the Hα we were unable to make a clear detection of Galactic [O I] emission toward HD 93521, despite using an "on-off" technique and repeating observations at different times of year. The incomplete subtraction of the very bright [O I] airglow line in each "on-off" spectrum prevented the detection of interstellar [O I] emission near the LSR. Although the intermediate velocity component near –50 km s^{-1} was adequately separated from both the airglow line and the prominent OH feature 115 km s^{-1} to the blue of the airglow line, the residual atmospheric line contamination in the "on-off" spectra led to baseline uncertainties that were comparable to or greater than the intensity of any Galactic emission present near –50 km s^{-1}.

Figure 4 shows three "on-off" [O I] spectra. The top panel is the 600 s average of the "off" (the Lockman Window) spectra in Data Sets 8a and 8b subtracted from the 600 s average of the HD 93521 spectra in the same Data Sets. The middle and bottom panels show spectra obtained similarly for Data Sets 9a,b and 11, respectively. An upper limit on the possible interstellar [O I] intensity is given in Table 5. This limit is based on fits to "on-off" spectra using data from Data Sets 8a through 11. For these fits, it was assumed that the Galactic [O I] emission was at –51 km s^{-1} (the velocity of the Hα emission) and had a width of 34 km s^{-1}. This width was calculated from the width of the Hα component at –51 km s^{-1} assuming that the Hα and [O I]-emitting gas is well-mixed and at a temperature of 8000 K. The Gaussian component shown in each of the spectra in Figure 4 illustrates one possible fit to the data. This component has a radial velocity fixed at –51 km s^{-1}(LSR), a width fixed at 34 km s^{-1} (FWHM), and an intensity slightly less than half the upper limit. For completeness, Table 5 includes [O I]/Hα intensity ratios for both the upper limit and sample fit cases. These intensity ratios incorporate a correction for the slight differences in instrument response (optical transmittance and detector quantum efficiency) between 6300 Å and 6563 Å.

4. DISCUSSION AND CONCLUSIONS

Interstellar Hα emission has been detected and characterized toward two high Galactic latitude, low H I column density sightlines, the Lockman Window ($\ell = 148\overset{\circ}{.}5$, $b = +53\overset{\circ}{.}0$) and HD 93521 ($\ell = 183\overset{\circ}{.}1$, $b = +62\overset{\circ}{.}2$). The relatively bright geocoronal line and the presence of many lower intensity, unidentified atmospheric emission lines make it difficult to

measure accurately the interstellar Hα emission in these faintest parts of the sky. However, from careful, long integration WHAM spectra spread over many months, the interstellar and terrestrial emissions were successfully separated. The results provide new constraints on the nature of the interstellar clouds along these two sightlines and their environment.

We have found that the Lockman Window, in addition to having the lowest H I column density in the sky (5×10^{19} cm^{-2}), also has unusually weak interstellar Hα emission (0.20 R), well below the 0.8 R average for this Galactic latitude (from the WHAM sky survey; Haffner et al. 2002). This region of the sky thus appears to be a true low column density window through the Galactic disk, depleted both in H I and in H II. Only one Hα velocity component is detected toward the Lockman Window, the component near the LSR, even though in the H I spectrum there is also a prominent emission component near –50 km s^{-1} (see Fig. 3). An Hα intensity of 0.20 R for the Lockman Window implies an emission measure of 0.55 cm^{-6} pc (at 10^4 K), which corresponds to a column density $N_{H\ II} \approx 2 \times 10^{19}$ cm^{-2}, if the mean density within the ionized regions is about 0.08 cm^{-3} (see Reynolds 1991). This is approximately 40% the H I column density and implies that the total hydrogen column density in this direction is about 7×10^{19} cm^{-2}.

Toward HD 93521, 21° away, the slow and intermediate velocity components detected in Hα clearly correspond to the two principal emission components present in the 21 cm spectrum. The intensity of the intermediate velocity (–50 km s^{-1}) component relative to the slow (–10 km s^{-1}) component is significantly weaker in the Hα spectrum than in the 21 cm spectrum, suggesting that perhaps an intermediate velocity Hα component toward the Lockman Window is just below the detection limit of the observation. For HD 93521 there is also strong evidence for a high velocity Hα emission component at –90 km s^{-1}, but no corresponding feature in the H I spectrum. This sightline is very near the High Velocity H I Cloud Complex M, parts of which have been detected in Hα at radial velocities ranging from –109 km s^{-1} to –61 km s^{-1} (Tufte et al. 1998). Therefore, the high velocity Hα component may be associated with a fully ionized portion of this high velocity cloud complex. The total Hα intensity (0.37 R) for the HD 93521 sightline corresponds to an emission measure of 1.0 cm^{-6} pc, and thus $N_{H\ II} \approx 4 \times 10^{19}$ cm^{-2} (about 30% of the H I column density of 1.25×10^{20} cm^{-2}).

Although there is good correspondence between the H II and H I for the low velocity and (for HD 93521) the intermediate velocity components, the difference in the general appearance of the Hα and 21 cm line profiles strongly suggests that the H II and the H I are not mixed together in the form of partially ionized clouds. In particular, the Hα components appear systematically broader. For example, the width (FWHM) of the intermediate velocity H I component toward HD 93521 is 20 km s^{-1}, only about half that of the corresponding

Hα emission. As a result, there is significant blending between the slow and intermediate velocity components in the Hα spectrum, whereas these components are well resolved in the H I spectrum. This is not a result of the different spectral resolutions of the Hα and 21 cm observations. Therefore, rather than being primarily neutral clouds that are 30%–40% ionized, as proposed by Spitzer & Fitzpatrick (1993) and Sciama (1998), each component seems to consist of separate regions of H I and H II at nearly the same radial velocity. This could be the result of either a close physical association between the H I and H II (McKee & Ostriker 1977) or large scale organized motions of the interstellar medium along this sightline (Walters & Cox 2001).

Because the [O I] λ6300/Hα intensity ratio is a probe of the hydrogen ionization fraction within the emitting gas (see §1), observations of [O I] provide a potentially rigorous test of these "mixed" versus "separated" models for the H I and H II in these clouds. Unfortunately, the [O I] spectrum, which only allows an upper limit on the intermediate velocity (–50 km s^{-1}) component (Table 5; see also §3.5), does not provide an unambiguous result. If the temperature is as low as 6000 K, as adopted by Spitzer & Fitzpatrick (1993) based on the widths of lines generally associated with H I clouds, then the [O I] observations are consistent with their model of primarily neutral clouds containing a 30% mixture of H^+. On the other hand, if the temperature is closer to 10,000 K, as recent observations of [S II] λ6717 and [N II] λ6584 suggest (Pifer et al, in preparation), then these [O I] results imply that the emitting regions are predominantly ionized (i.e., $n(H^+)/n(H_{\rm total}) > 0.6$). The [O I] limit is also just consistent with recent predictions of a supernova remnant ionization model for the HD 93521 sightline by Slavin, McKee, & Hollenbach (2000). Given the severe atmospheric line contamination of this region (worse than at Hα), it will be extremely difficult with ground-based observations to push the sensitivity limit of the [O I] observations down to the level of 0.03 R or lower needed to test these models more definitively.

If the clouds in these two sightlines are in fact ionized by an external flux of ionizing radiation, then the Hα intensity of each H I cloud is a measure of the incident ionizing flux. Specifically, the one-sided incident flux is 2.2×10^6 $I_{\rm H\alpha}$ photons cm^{-2} s^{-1}, for $I_{\rm H\alpha}$ in Rayleighs and a temperature of 10^4 K (e.g., Reynolds et al. 1995; Tufte et al. 1998). These observations therefore imply a variation in the intensity of the ambient ionizing flux, from less than 1.3×10^5 photons cm^{-2} s^{-1} at the intermediate velocity (–50 km s^{-1}) H I cloud in the Lockman Window to about 4.4×10^5 photons cm^{-2} s^{-1} for the low velocity clouds. The Hα intensity of the high velocity (–90 km s^{-1}) component toward HD 93521 gives a flux of 5×10^4 photons cm^{-2} s^{-1}; however, because there is no associated H I detected at this velocity, the H II is probably density bounded, and thus the derived value for the ionizing flux must be considered as a lower limit. If the higher velocity clouds are farther from the Galactic midplane than the lower velocity clouds (Kuntz & Danly 1996), these results

indicate a decrease in the ionizing flux with distance above the plane.

We thank Mark Quigley for his help with the observations and Trudy Tilleman for her on-site monitoring of Kitt Peak sky conditions during these observations. N. R. H. gratefully acknowledges support through a Barry M. Goldwater Scholarship from the Excellence in Education Foundation. This work, including the operation of WHAM, was funded by the National Science Foundation through grant AST96-19424.

REFERENCES

Haffner, L. M. 1999, Ph.D. Thesis, University of Wisconsin–Madison

Haffner, L. M., Reynolds, R. J., & Tufte, S. L. 1998, ApJ, 501, L83

Haffner, L. M., Reynolds, R. J., Tufte, S. L., Jaehnig, K. P., & Percival, J. W. 2002, in preparation

Hartmann, D., & Burton, W. B. 1997, Atlas of Galactic Neutral Hydrogen (Cambridge: Cambridge Univ. Press)

Jahoda, K., Lockman, F. J., & McCammon, D. 1990, ApJ, 354, 184

Kuntz, K. D., & Danly, L. 1996, ApJ, 457, 703

Lockman, F. J., Jahoda, K., & McCammon, D. 1986, ApJ, 302, 432

McKee, C. F., & Ostriker, J. P. 1977, ApJ, 218, 148

Meyer, D. M., Jura, M., & Cardelli, J. A. 1998, ApJ, 493, 222

Reynolds, R. J. 1991, ApJ, 372, L17

Reynolds, R. J., Hausen, N. R., Tufte, S. L., & Haffner, L. M. 1998, ApJ, 494, L99

Reynolds, R. J., Tufte, S. L., Kung, D. T., McCullough, P. M., & Heiles, C. 1995, ApJ, 448, 715

Sciama, D. W. 1998, ApJ, 505, L35

Slavin, J. D., McKee, C. F., & Hollenbach, D. J. 2000, ApJ, 541, 218

Spitzer, L., Jr., & Fitzpatrick, E. L. 1993, ApJ, 409, 299

Tufte, S. L. 1997, Ph.D. Thesis, University of Wisconsin–Madison

Tufte, S. L., Reynolds, R. J., & Haffner, L. M. 1998, ApJ, 504, 773

Walters, M. A. & Cox, D. P. 2001, ApJ, 549, 353

This preprint was prepared with the AAS LaTeX macros v5.0.

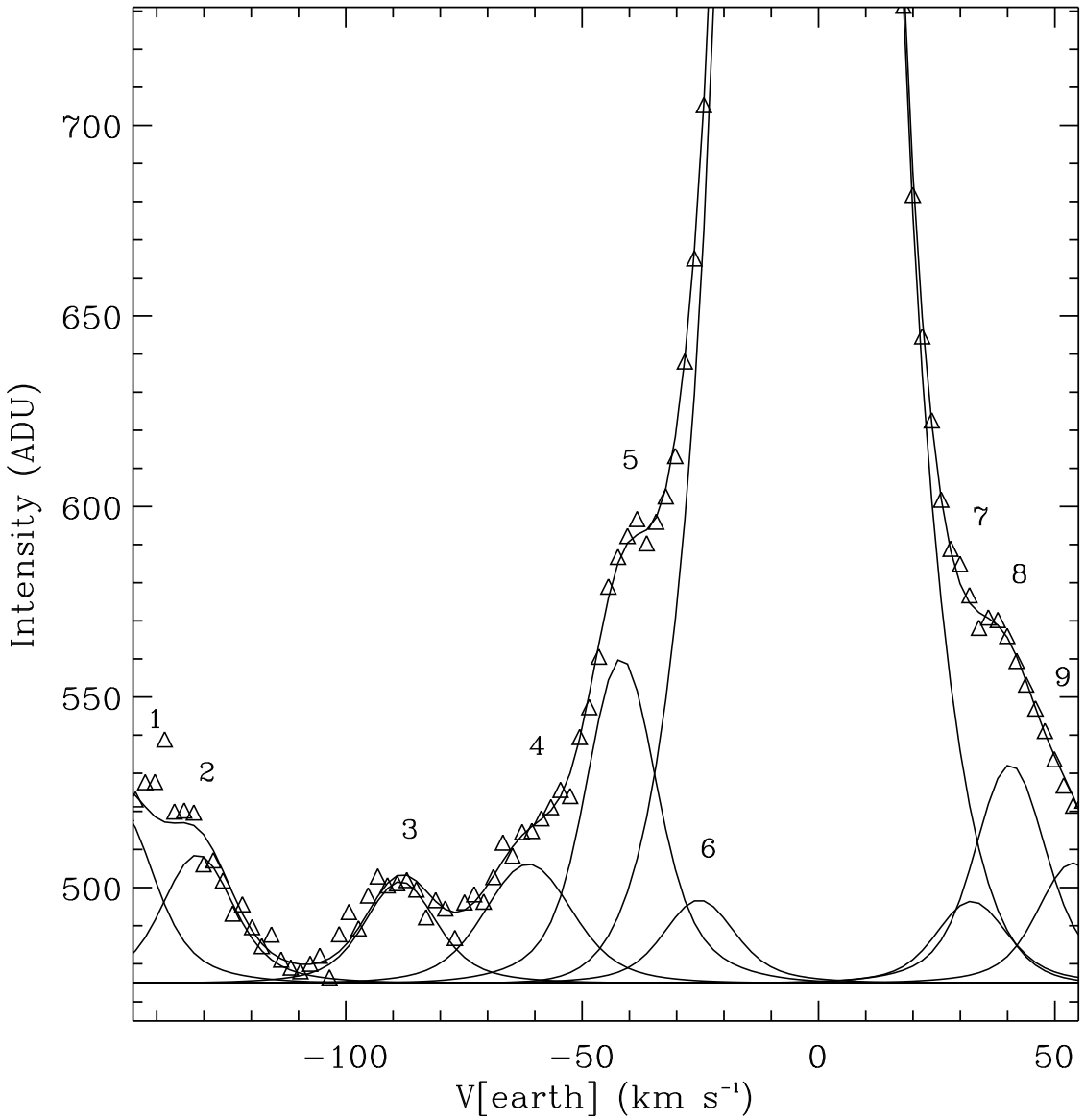

Fig. 1.— A spectrum of the faint atmospheric lines near Hα, with the geocoronal line positioned on the red side of the spectrum. The interstellar emission has been subtracted from this spectrum. The weak atmospheric lines are fit with solid lines and are numbered according to the line identifications in Table 3. The bright geocoronal line at –2 km s^{-1} with respect to the earth is also fit (the shift from zero is a fine structure effect, resulting from the fact that this line is not a recombination line). The solid line through the data points shows the composite fit. A 15 km s^{-1} wide line with an intensity of 0.1 R would have a peak height above background of about 92 arbitrary data units (ADU) on the intensity scale. The vertical scale has been expanded to show the weak atmospheric lines. The peak of the geocoronal line is at 4250 ADU.

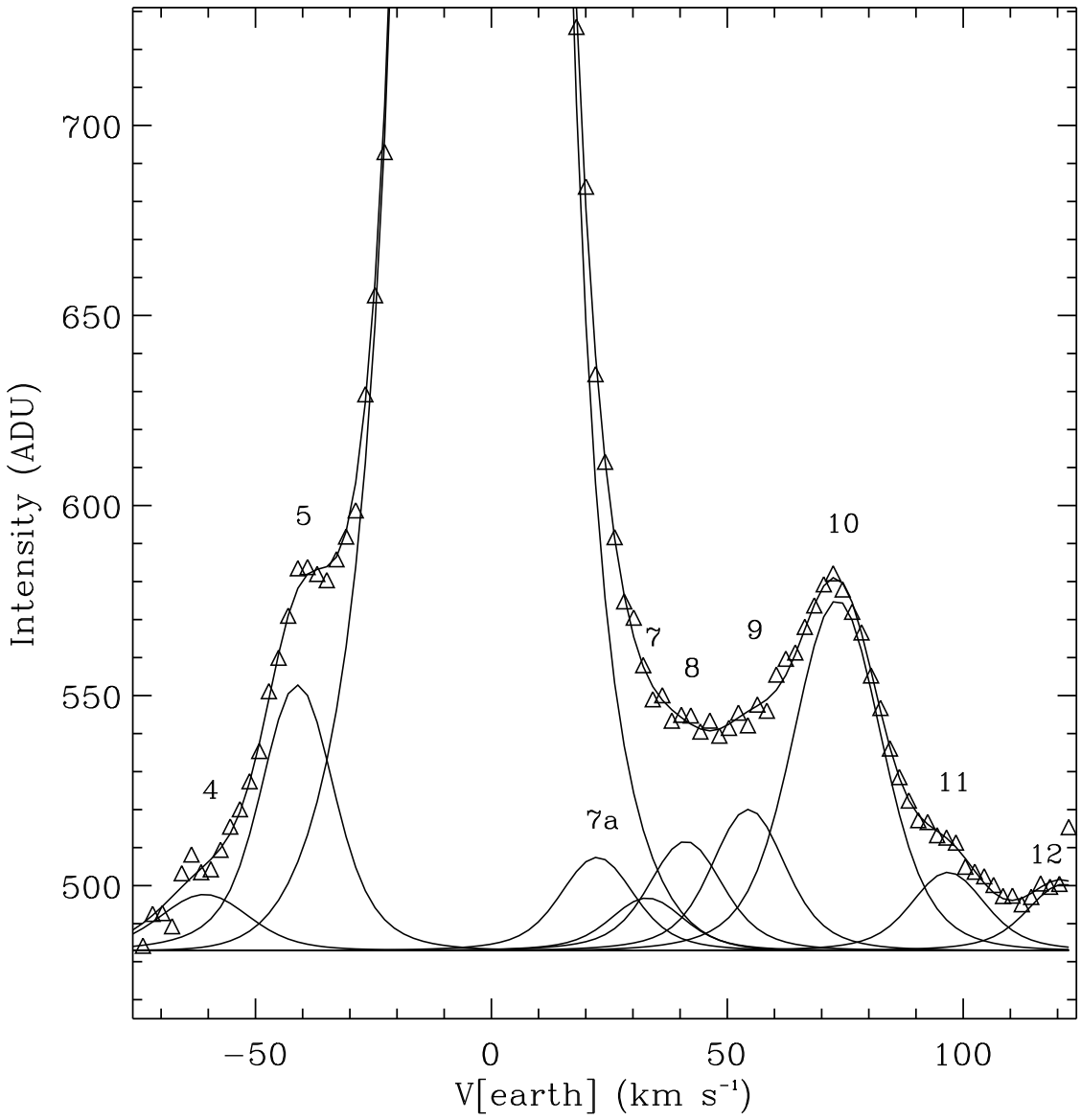

Fig. 2.— A spectrum of faint atmospheric lines near Hα similar to that in Figure 1, except the geocoronal line is positioned on the blue side of spectrum and the observations were taken at a different time of the year. The vertical scale matches that of Figure 1. The peak of the geocoronal line is at 3800 ADU.

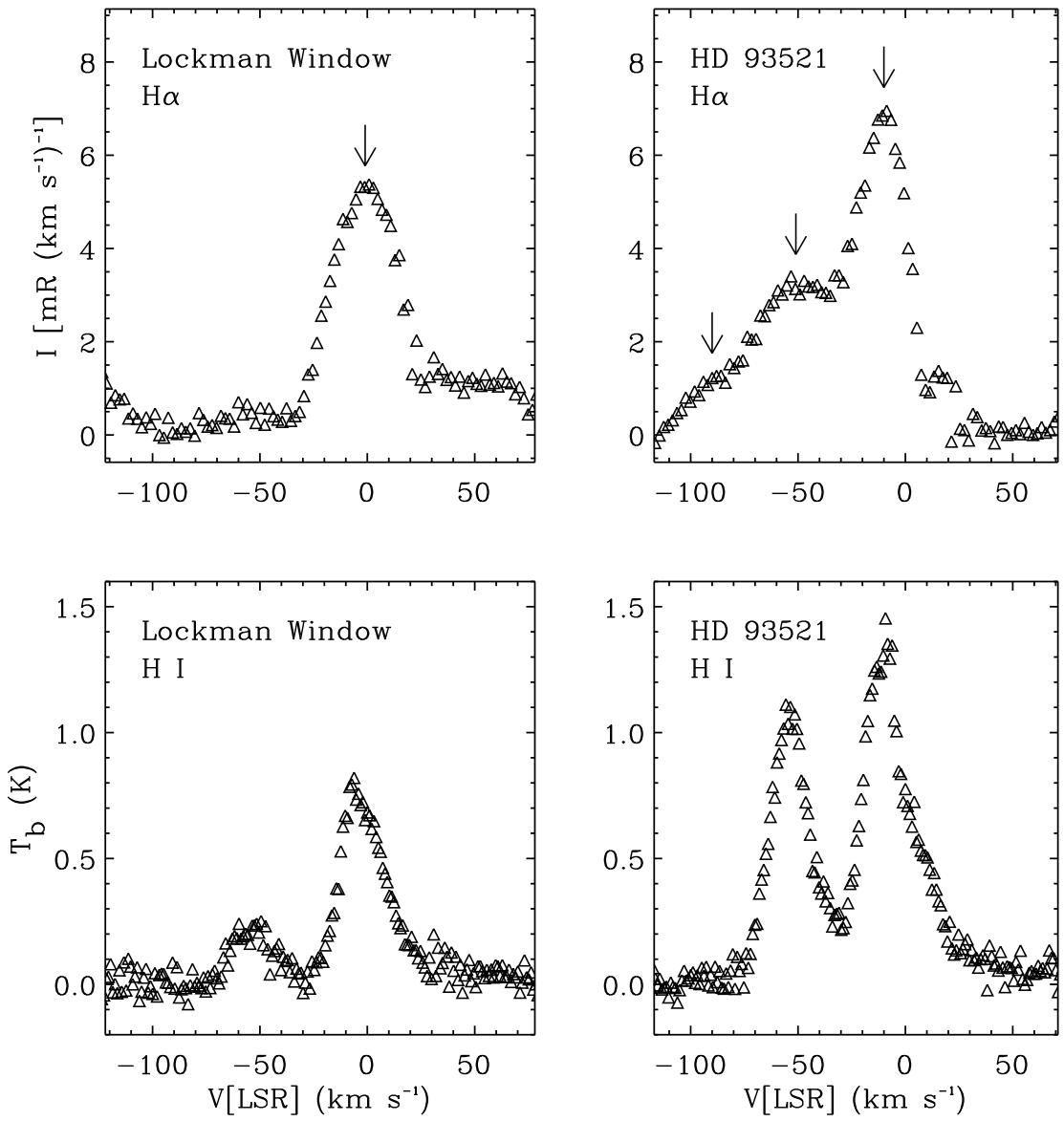

Fig. 3.— Hα and H I spectra toward the Lockman Window and HD 93521. The Hα data are "on-off" subtraction spectra with the residuals from the incompletely-subtracted geocoronal line removed (see text). The intensity scale for the Hα spectra is in milli-rayleighs (mR) per km s^{-1}. A constant was subtracted from the HD 93521 Hα spectrum in order to bring the background level to zero. Arrows mark the velocity of the detected emission components. The H I spectra are from the Leiden/Dwingeloo survey (Hartmann & Burton 1997).

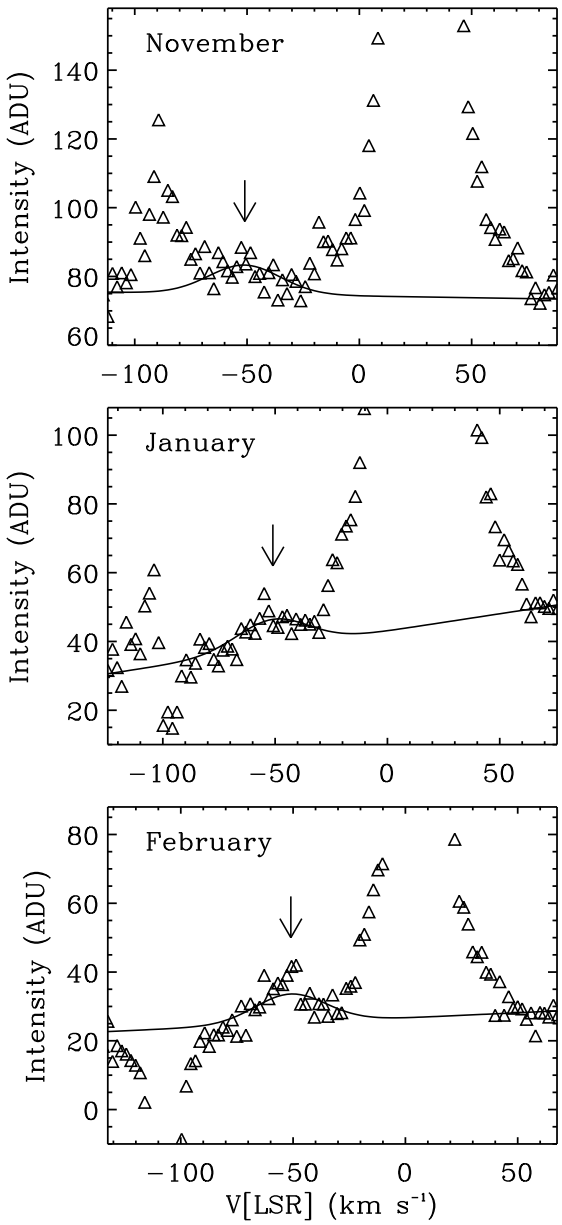

Fig. 4.— [O I] λ6300 spectra toward HD 93521. The spectra are "on-off" subtractions made from data gathered at three different times of year (details given in text). The Gaussian fit (solid line) through the data points in each panel is centered at the radial velocity of the corresponding Hα emission (marked with an arrow). This Gaussian has a width of 34 km s^{-1} and an intensity of 0.026 R (see text). A 34 km s^{-1} wide line with an intensity of 0.1 R would have a peak height above the baseline of about 30 ADUs on this intensity scale. In all three panels, the vertical scale has been expanded. In the top panel, the incompletely-subtracted [O I] airglow line, at +28 km s^{-1}(LSR), has a peak height of 1450 ADU. In the middle panel, the airglow line residual is at +14 km s^{-1} and peaks at 3240 ADU. In the bottom panel, the airglow line residual is at + 6 km s^{-1} and peaks at 825 ADU. The feature near –100 km s^{-1} in the three spectra is the incompletely-subtracted atmospheric OH line.

Table 1. List of Hα Observations

Data Set	Observation Date	Total Exposure Time (s) HD 93521 ($\ell = 183\overset{\circ}{.}1$, $b = +62\overset{\circ}{.}2$)	Lockman Window ($\ell = 148\overset{\circ}{.}5$, $b = +53\overset{\circ}{.}0$)	Off A ($\ell = 163\overset{\circ}{.}5$, $b = +53\overset{\circ}{.}5$)
1a	1997 Nov 5	1200	1200	···
1b	1997 Nov 7	1200	1200	···
1c	1997 Nov 8	600	600	···
2a	1998 Apr 22[a]	···	1800	···
2b	1998 Apr 23[a]	···	1800	···
3	1999 Jan 18	3000	6000[b]	···
4a	1999 Apr 16	···	600	···
4b	1999 Apr 20	···	600	···
5	1999 Dec 12	···	3600	3600
6	2000 Feb 2[a]	···	3600	3600
7	2000 Feb 4	3600	···	3600

[a]Spectra from this date have the geocoronal line positioned on the blue side of the 200 km s^{-1} spectral range.

[b]Individual spectra are 1200 s exposures.

Table 2. List of [O I] λ6300 Observations

Data Set	Observation Date	Total Exposure Time (s) HD 93521 ($\ell = 183\overset{\circ}{.}1$, $b = +62\overset{\circ}{.}2$)	Lockman Window ($\ell = 148\overset{\circ}{.}5$, $b = +53\overset{\circ}{.}0$)	Off A ($\ell = 163\overset{\circ}{.}5$, $b = +53\overset{\circ}{.}5$)
8a	1998 Nov 18	2400	1200	···
8b	1998 Nov 21	2400	1200	···
9a	1999 Jan 18	2400	2400[a]	···
9b	1999 Jan 22	2400	1200	···
10a	1999 Apr 16	1200	600	···
10b	1999 Apr 20	3600	1800	···
11	2000 Feb 4	2400	···	2400

[a]Individual spectra are 1200 s exposures.

Table 3. Faint Atmospheric Lines near Hα

Line[a]	Wavelength (Å)	Width[b] (km s^{-1})	Adopted Intensity (% of Line 5 Intensity)	Measured Intensity[c] (R)	
1	6559.55	10	54	0.070[e]	···
2	6559.92	10	24	0.052	···
3	6560.86	10	20	0.041	···
4	6561.45	15	33	0.057	0.027
5	6561.88	10	100	0.13	0.11
6	6562.25	10	30	0.033	···
7	6563.51	10	30	0.033	0.021
7a	6563.27[d]	10	···	···	0.038
8	6563.69	10	65	0.088	0.045
9	6563.98	10	39	0.048	0.058
10	6564.39	15	160	···	0.17
11	6564.90	10	36	···	0.032
12	6565.44	10	29	···	0.027

[a]Line numbers correspond to labels in Figure 1 and Figure 2.

[b]Fixed widths were adopted. See discussion in §3.1.

[c]Left column refers to line intensities in Figure 1, and right column refers to line intensities in Figure 2.

[d]Wavelength was determined from the spectrum in Figure 2 only.

[e]Intensity in the fit was fixed at 54% of Line 5 intensity.

Table 4. Hα Results

Direction	V_{LSR} (km s^{-1})	FWHM (km s^{-1})	I (R)
HD 93521	–10 ± 4	22 ± 6	0.20 ± 0.07
	–51 ± 3	39 ± 7	0.15 ± 0.03
	–90 ± 5	25[a]± 5	0.023 ± 0.009
Lockman Window	–1 ± 4	30 ± 5	0.20 ± 0.05
	(–54)[b,c]	(25)	< 0.06
Off A	(0)	(25)	< 0.11
	(–50)	(25)	< 0.06

[a]Fixed at this value during the fitting.

[b]Parentheses denote no Hα component detected.

[c]Velocity of the H I emission in the Lockman Window spectrum shown in Figure 3.

Table 5. [O I] λ6300 Results

Direction	V_{LSR} (km s^{-1})	FWHM (km s^{-1})	I (R)	$I([O\ I])/I(H\alpha)$ (energy units)	$n(H^+)/n(H^\circ)$ 6000 K	$n(H^+)/n(H^\circ)$ 10,000 K
HD 93521	(–51)[a,b]	(34)[c]	<0.060	<0.43	>0.13	>1.4
	(–51)	(34)	0.026[d]	0.18	0.32	3.3

[a]Parentheses denote no component detected.

[b]Velocity of the Hα emission component.

[c]Calculated based on the width of the Hα component and a gas temperature of 8000 K.

[d]Intensity of the gaussian fit in Figure 4.